J. Phys. Chem. A **2009,** *113,* 6121–6132 **6121**

Thermochemistry for the Dehydrogenation of Methyl-Substituted Ammonia Borane Compounds

Daniel J. Grant,[†] Myrna H. Matus,[†,‡] Kevin D. Anderson,[†] Donald M. Camaioni,[§]
Sharon R. Neufeldt,[⊥,¶] Clinton F. Lane,[⊥,#] and David A. Dixon*,[†]

Chemistry Department, University of Alabama, Shelby Hall, Box 870336, Tuscaloosa, Alabama 35487-0336,
Unidad de Servicios de Apoyo en Resolución Analítica, Universidad Veracruzana, A. P. 575,
Xalapa, Veracruzana, México, Fundamental Sciences Division, Pacific Northwest National Laboratory,
P.O. Box 999, Richland, Washington 99352, and Department of Chemistry and Biochemistry, Northern Arizona
University, South Beaver Street, Building 20, Room 125, Flagstaff, Arizona 86011-5698

Received: March 11, 2009; Revised Manuscript Received: March 29, 2009

Atomization energies at 0 K and heats of formation at 0 and 298 K are predicted for $(CH_3)H_2N{-}BH_3$, $(CH_3)HN{=}BH_2$, $(BH_3)HN{=}CH_2$, $(CH_3)H_2B{-}NH_3$, $(CH_3)HB{=}NH_2$, and $(NH_3)HB{=}CH_2$, as well as various molecules involved in the different bond-breaking processes, from coupled cluster theory (CCSD(T)) calculations. In order to achieve near-chemical accuracy (±1 kcal/mol), three corrections were added to the complete basis set binding energies based on frozen core CCSD(T) energies, corrections for core−valence, scalar relativistic, and first-order atomic spin−orbit effects. Scaled vibrational zero-point energies were computed with the MP2 method. The heats of formation were predicted for the respective dimethyl- and trimethyl-substituted ammonia boranes, their dehydrogenated derivatives, and the various molecules involved in the different bond breaking processes, based on isodesmic reaction schemes calculated at the G3(MP2) level. Thermodynamics for dehydrogenation pathways in the monomethyl-substituted molecules were predicted. Dehydrogenation across the B−N bond is more favorable as opposed to dehydrogenation across the B−C and N−C bonds. Methylation at N reduces the exothermocity of the dehydrogenation reaction and makes the reaction more thermoneutral, while methylation at B moves it away from thermoneutral. Various mixtures of $CH_3NH_2BH_3$ and NH_3BH_3 were made, and their melting points were measured. The lowest melting mixture contained ∼35% NH_3BH_3 by weight and melted at 35−37 °C.

Introduction

There is substantial interest in the discovery of new molecules for chemical hydrogen storage systems in which dehydrogenation (hydrogen release) and hydrogenation (regeneration of spent fuel) from these molecules are near-thermoneutral processes. The need for a thermoneutral reaction arises because one wants to minimize the heat needed for the reaction to release hydrogen and to minimize the energy requirements of the regeneration process. An important potential chemical hydrogen storage material is ammonia borane, and there are a number of efforts focused on its use for H_2 storage.[1−9] High-level ab initio molecular orbital theory has been used to predict reliably the gas-phase thermochemistry of ammonia borane and various dehydrogenation processes[10] as well as for the heats of formation of larger $B_xN_yH_z$ compounds.[11]

An issue with ammonia borane is that it is a solid at room temperature, and this may make use of the fuel in the transportation sector difficult as the use of solids as a fuel is not currently practiced. Solid fuels would require substantial changes to the infrastructure. Ammonia borane is a solid due to the large number of moderate-strength intermolecular H···H bonds formed between the $H^{\delta+}$ on the N and the $H^{\delta-}$ on the B.[12−14] Alkyl-substituted ammonia boranes have lower melting points than does ammonia borane[15] presumably because there are fewer H···H interactions due to the presence of the alkyl groups. It has recently been found that borane amine can be solubilized in methyl-substituted ammonia borane (see below).[16] Dimethylamine borane has a melting point of 36 °C,[17] and a melt of the neat compound can be kept at 45 °C for 7 days with no observed decomposition.[18] The vapor pressures of the *N*-methyl-substituted methylamine boranes have been reported, and the heats of sublimation for the *N*-mono and *N*,*N*-dimethyl derivatives are higher than that of the *N*,*N*,*N*-trimethyl derivative.[19] Thus, addition of methyl-substituted ammonia boranes could enable the generation of a liquid fuel and potentially enable use of portions of the current infrastructure. As there is a weight penalty associated with any additional components, we wished to determine if the substituted ammonia boranes can also act as a hydrogen source in terms of their thermodynamic properties. *N*-Methylammonia borane and ammonia *B*-methylborane have a weight percent storage for hydrogen of 9.8% if two molecules of H_2 are produced as compared to the amine boranes having 14.9% if two molecules of H_2 are produced. This requires that we know the thermochemistry for the dehydrogenation of *N*-methylammonia borane and ammonia *B*-methylborane to see if the weight issues can be improved. As the thermodynamic properties are not known, we have used high-level molecular orbital theory to predict the critical heats of formation. The heats of formation of these simple model

---

* To whom correspondence should be addressed. E-mail: dadixon@bama.ua.edu.

[†] University of Alabama.

[‡] Universidad Veracruzana.

[§] Pacific Northwest National Laboratory.

[⊥] Northern Arizona University.

[¶] Current address: Department of Chemistry, University of Michigan, 930 N. University, Ann Arbor, MI 48109-1055.

[#] Deceased May 19, 2007.

10.1021/jp902196d CCC: $40.75

compounds are also needed accurately for use in isodesmic reaction schemes in order to predict the heat of formation of larger molecules. In the current work, we have calculated the heats of formation for the *N*-methylammonia borane and ammonia *B*-methylborane, as well as various molecules involved in the dehydrogenation processes ($(CH_3)H_2N-BH_3$, $(CH_3)H_2B-NH_3$, $(CH_3)HN{=}BH_2$, $(BH_3)HN{=}CH_2$, $(CH_3)HB{=}NH_2$, and $(NH_3)HB{=}CH_2$) at the CCSD(T)/CBS level (coupled cluster with an approximate triples correction[20] at the complete basis set limit). In addition, we report G3(MP2) calculations on the alkylated dehydrogenated products derived from cyclodi-, cyclotri-, and cyclotetraborazane.

In order to further understand the chemistry of these compounds in terms of their reactivity and stability, we are also interested in the various σ- and π-bond dissociation energies (BDEs). The B−N dative bond in H_3B-NH_3 is 27.2 kcal/mol[10] as compared to the covalent C−C σ-bond energy of 90.1 kcal/mol at 298 K for C_2H_6.[21] We have previously investigated the σ- and π-bonds in the main Group IIIA−Group VA $H_2A{=}XH_2$ compounds and calculated the rotation barrier to estimate the π-bond energies.[22] The bond energies could then be compared to the σ- and π-bond energies in C_2H_4, which has a covalent π-bond.[23] We predicted that the adiabatic σ-bond strength of $H_2B{=}NH_2$ of 109.8 kcal/mol was comparable to the adiabatic σ-bond strength in $H_2C{=}CH_2$ of 106 kcal/mol, given the experimentally determined π-bond strength of 65 kcal/mol[24] and an adiabatic C=C BDE of 171 kcal/mol.[21] In addition, we defined intrinsic π-bond strengths that are corrected for pyramidalization in the ground-state and rotated transition-state structures. The adiabatic σ-bond strengths for $H_2B{=}NH_2$ and $H_2Al{=}NH_2$ did not change substantially when considering the intrinsic π-bond strength due to the rather small inversion barriers at N in the rotated transition-state structures.

There have been a number of experimental investigations of the structures of the *N*-methyl-substituted ammonia boranes. Bauer[25] used electron diffraction to study the structure of *N*-trimethylamine borane. Later, Taylor et al.[26] used microwave spectroscopy to obtain the B−N and C−N bond distances and the CNB angle of trimethylamine borane. The best molecular structure of trimethylamine borane was obtained from a combination of gas-phase electron diffraction and microwave spectroscopy data by Shibata et al.[27] Bowden et al. reported the crystal structure of methylamine borane and showed that thermal decomposition of the melt starting at ~100 °C leads to liberation of H_2;[28] a second H_2 is lost near 190 °C. Most recently, Wann et al.[29] reported an elaborate detailed study of the structures of methylamine borane and dimethylamine borane by X-ray diffraction of the crystal and gas-phase electron diffraction aided by quantum chemical calculations. Anane et al. reported G2(MP2) B−N bond energies for the $(CH_3)_nH_{3-n}BNH_3$ and $BH_3N(CH_3)_nH_{3-n}$ ($n = 0-3$) complexes.[30,31] Gilbert compared density functional theory (DFT) with different exchange correlation functionals with MP2 all with the 6-311++G(d,p) basis set and experiment for different BR_3-NR_3' compounds. He found that MP2 gives the best agreement with experiment.[32] Very recently, Sun et al. reported the B−N BDEs for BH_3NH_3, $BH_3NH_2CH_3$, and $BH_3NH(CH_3)_2$ at the B3LYP/6-311G** and MP2/6-31G** levels as well as the barrier height for the unimolecular loss of H_2. The barrier heights are predicted to increase slightly upon methylation at the MP2/6-31G* level.[33]

Experimental Methods

Synthesis of Ammonia Borane. ***Procedure 1: Addition of $BH_3 \cdot THF$ to NH_3.*** Ammonia (8 mL, 320 mmol) was condensed into a cold (−78 °C) graduated cylinder and then allowed to warm slowly. The NH_3 gas was bubbled into THF (50 mL) in a flask held at −40 °C under N_2. To this solution was added 1 M $BH_3 \cdot THF$ (100 mL, 100 mmol), and the reaction mixture was cooled to −78 °C and stirred for 1 h. After slow warming to ambient temperature, the reaction mixture was concentrated by using a rotary evaporator and dried under vacuum to yield an oily white solid. This was stirred in isopropyl alcohol, filtered, and dried under vacuum to yield 2.04 g (66%) of a white solid.

Procedure 2: Addition of NH_3 to $BH_3 \cdot THF$. Ammonia (5 mL, 200 mmol) was condensed into a cold (−78 °C) graduated cylinder and then allowed to warm slowly. The gas was bubbled into 1 M $BH_3 \cdot THF$ (100 mL, 100 mmol) in a flask held at −20 °C under N_2. The reaction mixture was stirred for 1 h at −20 °C, then allowed to warm to ambient temperature, and stirred overnight. The reaction mixture was filtered through diatomaceous earth and concentrated by using a rotary evaporator and then dried under vacuum to yield an oily white solid. This was stirred in isopropyl alcohol, filtered, and dried under vacuum to yield 1.23 g (40%) of a white solid.

Synthesis of Methylamine Borane. Methylamine (21.3 mL, 480 mmol) was condensed into a cold (−78 °C) graduated cylinder and then allowed to warm slowly. The gas was bubbled into 1 M $BH_3 \cdot THF$ (400 mL, 400 mmol) in a flask held at −20 °C under N_2. The reaction mixture was then allowed to slowly warm to ambient temperature and stirred for 2 h. The reaction mixture was concentrated by using a rotary evaporator and dried under vacuum to yield an oily white solid. This was stirred in *n*-heptane, filtered, and dried under vacuum to yield 16.34 g (91%) of a white solid.

Cosynthesis of Ammonia and Methylamine Borane. The ratios of ammonia and methylamine used in the cosynthesis were chosen to yield a mixture of 20−40% ammonia borane in methylamine borane. The experimental yields from the procedures described above for the individual syntheses of ammonia borane and methylamine borane indicated that the reaction of the two amines with $BH_3 \cdot THF$ did not proceed to the same degree of completion. Ammonia (1.8 mL, 70 mmol) was condensed into a cold (−78 °C) graduated cylinder and then allowed to warm slowly. The gas was bubbled into 1 M $BH_3 \cdot THF$ (100 mL, 100 mmol) in a flask held at −40 °C under N_2. Methylamine (3.2 mL, 72 mmol) was then condensed into a cold (−78 °C) graduated cylinder and allowed to warm slowly. The gas was bubbled into the reaction mixture at −15 °C under N_2. The reaction mixture was allowed to warm slowly to ambient temperature and stirred for 1 h. The reaction mixture was concentrated by using a rotary evaporator and then dried under vacuum to yield an oily white solid. The solid melted completely in a 30 °C water bath and separated into two liquid layers. The top layer was isolated and determined to be a mixture of about 30−40% ammonia borane in methylamine borane by ^1H NMR. The bottom layer was mainly impurities and side products (including *n*-butanol due to ring opening of the THF) by NMR.

Melting of Ammonia Borane and Methylamine Borane Mixtures. Eleven mixtures of ammonia borane (AB) and methyl amine borane (MeAB) were prepared in weight ratios ranging from 0:1 to 1:0 of AB/MeAB. One gram of each mixture was prepared by combining the appropriate amount of AB and MeAB in a test tube; each mixture was then suspended in THF (10 mL) and poured into a crystallizing dish. After evaporation of the THF, the resulting white solid was dried under vacuum.

Multiple melting point capillary tubes were prepared for each mixture. Each tube was evacuated, refilled with N_2 (3×), and sealed with paraffin wax. Melting ranges were obtained by using a Meltemp device set to a specific temperature. Melting was observed 15 s after insertion of the capillary tube. Multiple temperatures were tested for each AB/MeAB mixture using a different capillary tube for each temperature setting.

Computational Methods

We have been developing a composite approach[34,35] to the prediction of the thermodynamic properties of molecules based on molecular orbital theory using coupled cluster methods at the CCSD(T) level. In most CCSD(T) calculations of atomization energies (or heats of formation), the largest source of error typically arises from the finite basis set approximation, unless there is significant multireference character to the wave function. Our composite approach for predicting atomization energies makes use of the systematic convergence properties of the valence correlation-consistent family of basis sets including additional diffuse functions.[36] These basis sets are conventionally denoted as aug-cc-pVnZ, with n = D, T, and Q. The standard aug-cc-pVnZ basis sets were used for H, B, C, and N. We use the shorthand notation of aVnZ and VnZ to denote the aug-cc-pVnZ and cc-pVnZ basis sets, respectively, on H, B, C, and N. Only the spherical component subset (e.g., five-term d functions, seven-term f functions, etc.) of the Cartesian polarization functions were used. All CCSD(T) calculations were performed with the MOLPRO-2002 program system[37] on the Cray XD-1, Altix, or DMC at the Alabama Supercomputer Center or with a Dell Cluster at the University of Alabama.

For the open-shell atomic calculations, we used the restricted method for the starting Hartree–Fock wave function and then relaxed the spin restriction in the coupled cluster portion of the calculation. This method is conventionally labeled R/UCCSD(T). Our CBS estimates use a mixed exponential/Gaussian function of the form[38]

$$E(n) = E_{\mathrm{CBS}} + B\mathrm{e}^{-(n-1)} + C\mathrm{e}^{-(n-1)^2} \tag{1}$$

where $n = 2$ (aVDZ), 3 (aVTZ), and 4 (aVQZ). This extrapolation method has been shown to yield atomization energies in the closest agreement with experiment (by a small amount) as compared to other extrapolation approaches up through $n = 4$.

Most correlated electronic structure calculations based on molecular orbital theory are done in the frozen core approximation with the energetically lower lying orbitals, for example, the 1s in carbon, excluded from the correlation treatment. In order to achieve thermochemical properties within ±1 kcal/mol of experiment, it is necessary to account for core–valence correlation energy effects. Core–valence (CV) calculations were carried out with the weighted core–valence basis set cc-pwCVTZ.[39]

Two adjustments to the total atomization energy (TAE = ΣD_0) are necessary in order to account for relativistic effects in atoms and molecules. The first correction lowers the sum of the atomic energies (decreasing TAE) by replacing energies that correspond to an average over the available spin multiplets with energies for the lowest multiplets as most electronic structure codes produce only spin multiplet averaged wave functions. The atomic spin–orbit corrections are $\Delta E_{\mathrm{SO}}(\mathrm{B}) = 0.03$ kcal/mol and $\Delta E_{\mathrm{SO}}(\mathrm{C}) = 0.09$ kcal/mol from the tables of Moore.[40] A second relativistic correction to the atomization energy accounts for molecular scalar relativistic effects, ΔE_{SR}. We evaluated ΔE_{SR} by using expectation values for the two dominant terms in the Breit–Pauli Hamiltonian, the so-called mass–velocity and one-electron Darwin (MVD) corrections from configuration interaction singles and doubles (CISD) calculations.[41]The quantity ΔE_{SR} was obtained from CISD wave function with a VTZ basis set at the appropriate CCSD(T) or MP2 optimized geometry. The CISD(MVD) approach generally yields ΔE_{SR} values in good agreement (±0.3 kcal/mol) with more accurate values from, for example, Douglass–Kroll–Hess calculations,[42] for most molecules.

Geometries for the smaller molecules ($HBNH_2$, $HNBH_2$, $HBCH_2$, and $HNCH_2$) were optimized at the CCSD(T) level with the aVDZ and aVTZ basis sets. The geometry obtained with the aVTZ basis set was then used in a single-point aVQZ calculation. For the larger molecules, geometries were optimized at the MP2/VTZ level.[43,44] Geometries obtained with the VTZ basis set were then used in CCSD(T) single-point calculations with the aVDZ, aVTZ, and aVQZ basis sets. The impact of the use of the different geometries is on the order of a few tenths of a kcal/mol for these well-behaved systems. The zero-point energies (ΔE_{ZPE}) were obtained at the MP2 level with the VTZ basis set. To calculate the zero-point correction and account for anharmonic effects, the calculated harmonic A–H stretching frequencies were scaled by factors of 0.974 (B), 0.972 (C), and 0.973 (N), obtained by taking the average of the MP2/VTZ and experimental values[45−47] for the A–H stretches of BH_3, CH_4, and NH_3 and dividing the average by the theoretical value, respectively.

By combining our computed ΣD_0 values given by the following expression

$$\Sigma D_0 = \Delta E_{\mathrm{elec}}(\mathrm{CBS}) - \Delta E_{\mathrm{ZPE}} + \Delta E_{\mathrm{CV}} + \Delta E_{\mathrm{SR}} + \Delta E_{\mathrm{SO}} \tag{2}$$

with the known[48] heats of formation at 0 K for the elements, $\Delta H_{\mathrm{f}}^0(\mathrm{H}) = 51.63$ kcal/mol, $\Delta H_{\mathrm{f}}^0(\mathrm{B}) = 135.10$ kcal/mol,[49] $\Delta H_{\mathrm{f}}^0(\mathrm{C}) = 169.98$ kcal/mol, and $\Delta H_{\mathrm{f}}^0(\mathrm{N}) = 112.53$ kcal/mol, we can derive ΔH_{f}^0 values for the molecules under study. We employ what we consider to be the best heat of formation[49] of the boron atom, which has changed over time.[48,50−52] This value is based on W4 calculations of the total atomization energies of BF_3 and B_2H_6 and their experimental heats of formation.[53,54] Heats of formation at 298 K were obtained by following the procedures outlined by Curtiss et al.[55]

We have also calculated heats of formation and dehydrogenation energies employing a computationally less intensive approach by using the G3(MP2) level of theory[56] as it can be used for much larger molecules and we wish to test it.

Experimental Results

Various mixtures of $CH_3NH_2BH_3$ and NH_3BH_3 were made, and their melting points were measured as described above. The results are shown in Figure 1 (detailed values are given in Supporting Information). The lowest melting mixture contained ~35% NH_3BH_3 by weight and melted at 35–37 °C. As shown in Figure 1, a range of NH_3BH_3 weight percents from 20 to 50% in $CH_3NH_2BH_3$ will melt between 35 and 42 °C. The pure NH_3BH_3 melted at 118–120 °C, and pure $CH_3NH_2BH_3$ melted at 58–59 °C.

Computational Results

The calculated geometries for the molecules under study are given as Supporting Information in Tables SI-2 and SI-3, and the calculated harmonic frequencies are given in Table SI-4 of the Supporting Information, where they are compared with the

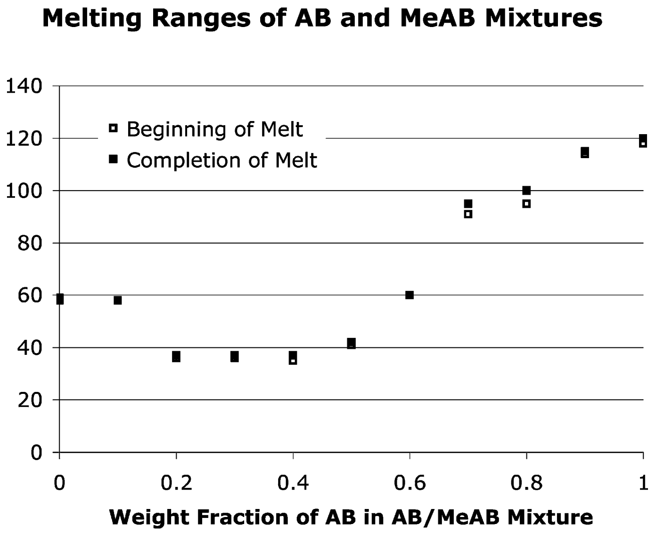

Figure 1. Melting temperature ranges in °C of ammonia borane/methylamine borane mixtures as a function of the weight percent of ammonia borane.

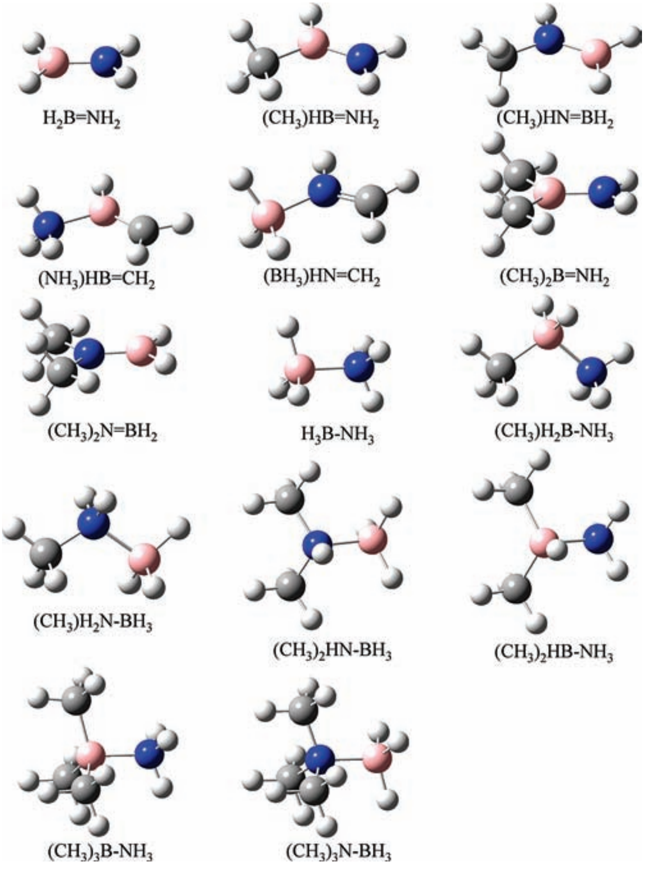

Figure 2. Optimized molecular structures for $H_2B{=}NH_2$, $(CH_3)HB{=}NH_2$, $(CH_3)HN{=}BH_2$, $(NH_3)HB{=}CH_2$, $(BH_3)HN{=}CH_2$, $(CH_3)_2B{=}NH_2$, $(CH_3)_2N{=}BH_2$, $H_3B{-}NH_3$, $(CH_3)H_2B{-}NH_3$, $(CH_3)H_2N{-}BH_3$, $(CH_3)_2HB{-}NH_3$, $(CH_3)_2HN{-}BH_3$, $(CH_3)_3B{-}NH_3$, and $(CH_3)_3N{-}BH_3$.

available experimental values. The total energies used in this study are also given as Supporting Information (Table SI-5). Optimized structures for the compounds with one B and N are shown in Figure 2.

Geometries and Frequencies. Structural data are available for a few of the molecules under study, and our calculated values are in excellent agreement with the reported values. We use the values calculated at the MP2/VTZ level in our discussion below unless specified otherwise. The lower-level MP2(full)/6-31G(*d*) values from the G2(MP2) calculations[30,31] for the free methylboranes and methylamines are in good agreement with our higher-level values. The C−N bond distance in $H_2C{=}NH$ is calculated to be 0.002 Å longer than the experimental value of 1.273 Å,[57] consistent with our prior calculations.[58]

For the free methyl-substituted boranes, the B−C bond distance in methylborane is predicted to increase by 0.007 and 0.002 Å, respectively, for dimethylborane and trimethylborane. A small decrease in the B−C bond distance of 0.003 Å is predicted for the dimethylborane radical $B(CH_3)_2$.

In the free methyl-substituted amines, the C−N bond distance in methylamine is calculated to be slightly shorter by 0.008 Å than the experimental value of 1.471 Å,[57] consistent with our prior calculations.[59] The C−N bond distances in dimethylamine and trimethylamine are predicted to be shorter by 0.01 and 0.001 Å than the experimental values of 1.464 and 1.451 Å, respectively.[57] Sequential methylation of methylamine leads to a further decrease in the C−N bond distance by 0.009 and 0.013 Å for $HN(CH_3)_2$ and $N(CH_3)_3$, respectively. An even larger decrease in the C−N bond distance of 0.025 Å is predicted for the dimethylamine radical $N(CH_3)_2$.

The effect of mono- and dimethyl substitution in $H_2B{=}NH_2$ at B for $(CH_3)HB{=}NH_2$ and $(CH_3)_2B{=}NH_2$ is predicted to increase the B−N bond distance by 0.005 and 0.010 Å, respectively, compared to the B−N bond distance in $H_2B{=}NH_2$. Sequential methylation at N leads to decreases in the B−N bond distance of 0.002 and 0.001 Å for $(CH_3)HN{=}BH_2$ and $(CH_3)_2N{=}BH_2$. The effect of ammoniation on the B−C bond distance in $(NH_3)HB{=}CH_2$ increases the bond distance by 0.043 Å as compared to that of $HB{=}CH_2$. We predict the equivalent borane substituent to have essentially no effect on the N−C bond distance in $(BH_3)HN{=}CH_2$ as compared to that of $HN{=}CH_2$.

Similarly, we can examine the effect of methylation at B and N on the B−N bond distance of $H_3B{-}NH_3$. Our calculated MP2/VTZ parameters for $(CH_3)H_2N{-}BH_3$ and $(CH_3)_2HN{-}BH_3$ are in reasonable agreement with the new experimental[29] data and the other MP2 optimizations.[29−31] The B−N bond distances of $(CH_3)H_2N{-}BH_3$ and $(CH_3)_2HN{-}BH_3$ are predicted to be 0.033 and 0.015 Å longer than the gas-phase electron diffraction (GED) refined values ($r_{a3,1}$) of 1.602(7) and 1.615(4) Å, respectively.[29] The N−C bond distances are also predicted to be slightly longer than the GED $r_{a3,1}$ values[29] by 0.025 and 0.0064 Å, respectively. Our calculated geometry parameters are also in excellent agreement with the MP2/aVQZ[29] values. For $(CH_3)H_2N{-}BH_3$ and $(CH_3)_2HN{-}BH_3$, our VTZ B−N and N−C bond distances are longer than the aVQZ values by an average of 0.011 and 0.006 Å, respectively. Our calculated parameters for trimethylamineborane, $(CH_3)_3N{-}BH_3$, are consistent with the experimental structural data.[25−27,29,57] The experimental B−N bond distances vary over ∼0.04 Å, and our calculated value is 0.022 Å shorter, 0.004 Å shorter, and 0.0144 Å longer than the experimental values of 1.656 ± 0.002 ($r_{a3,1}$),[27] 1.638 ± 0.01,[26,57] and 1.62 ± 0.15[25] Å determined from GED and spectroscopic data, microwave (MW) spectroscopy, and electron diffraction, respectively. The C−N and B−H bond distances are in good agreement with the recent experimental values.[25−27,57] Sequential methylation at B in $(CH_3)H_2B{-}NH_3$, $(CH_3)_2HB{-}NH_3$, and $(CH_3)_3B{-}NH_3$ leads to respective increases of 0.005, 0.013, and 0.021 Å in the B−N bond distance compared to that of $H_3B{-}NH_3$. Sequential methylation of $H_3B{-}NH_3$ at N leads to respective decreases in the B−N bond distance of 0.016, 0.021, and 0.017 Å for $(CH_3)H_2N{-}BH_3$, $(CH_3)_2HN{-}BH_3$, and

TABLE 1: Components for CCSD(T) Atomization Energies (kcal/mol)[a]

molecule	CBS[b]	ΔE_{ZPE}[c]	ΔE_{CV}[d]	ΔE_{SR}[e]	ΔE_{SO}[f]	ΣD_0 (0 K)[g]
$HBCH_2$ (C_{2v}−$^1A_1$)	425.62	20.68	2.12	−0.23	−0.12	406.74
$HBNH_2$ (C_s−$^2A'$)	387.92	22.83	1.66	−0.38	−0.03	366.34
$HNBH_2$ (C_1−^2A)	377.03	19.24	1.79	−0.31	−0.03	359.24
$HNCH_2$ (C_s−$^1A'$)	437.76	24.86	1.39	−0.38	−0.09	413.81
$HBCH_3$ (C_1−^2A)	476.35	27.78	1.97	−0.26	−0.12	450.16
$HBNH_3$ (C_1−^1A)	399.87	29.14	1.12	−0.33	−0.03	371.48
$HBNH_3$ (C_s−$^3A''$)	392.86	30.19	1.56	−0.40	−0.03	363.80
$HNBH_3$ (C_1−^3A)	392.74	23.55	1.84	−0.26	−0.03	370.73
$HNCH_3$ (C_s−$^2A''$)	472.95	30.74	1.37	−0.39	−0.09	443.10
H_2BCH_3 (C_s−$^1A'$)	586.05	34.87	2.15	−0.26	−0.12	552.95
$(CH_3)HB{=}NH_2$ (C_s−$^1A'$)	803.56	47.93	2.99	−0.59	−0.12	757.91
$(NH_3)HB{=}CH_2$ (C_s−$^1A'$)	755.99	48.07	2.94	−0.57	−0.12	710.16
$(CH_3)HN{=}BH_2$ (C_s−$^1A'$)	785.93	48.01	2.95	−0.60	−0.12	740.16
$(BH_3)HN{=}CH_2$ (C_s−$^1A'$)	752.61	46.16	2.89	−0.53	−0.12	708.69
$(CH_3)H_2B{-}NH_3$ (C_s−$^1A'$)	909.48	61.73	3.02	−0.59	−0.12	850.06
$(CH_3)H_2N{-}BH_3$ (C_s−$^1A'$)	897.94	61.84	2.98	−0.61	−0.12	838.24

[a] The atomic asymptotes were calculated with the R/UCCSD(T) method. [b] Extrapolated by using eq 1 with the aVDZ, aVTZ, and aVQZ basis sets. [c] The zero-point energies were taken as 0.5, the sum of the MP2 scaled frequencies. [d] Core−valence corrections were obtained with the cc-pwCVTZ (B, C, N) basis sets at the optimized CCSD(T)/aVTZ or MP2/VTZ geometries. [e] The scalar relativistic correction is based on a CISD(FC)/VTZ MVD calculation. [f] Correction due to the incorrect treatment of the atomic asymptotes as an average of spin multiplets. Values are based on C. Moore's Tables, ref 40. [g] The theoretical value of ΔD_0 (0 K) was computed from the CBS estimates.

$(CH_3)_3N{-}BH_3$ compared to that of $H_3B{-}NH_3$. Thus, the B−N bond distance in $(CH_3)_3N{-}BH_3$ is longer than that in $(CH_3)_2HN{-}BH_3$, consistent with the MP2(full)/6-311++G**[29] and MP2(full)/6-31G(*d*)[30,31] calculations. The available experimental data[29] suggests that methylation at N will decrease the B−N bond distance for the first methyl group, and then, subsequent methylation at N will increase the B−N bond distance. Further experimental results are needed to explain the discrepancy in the trend.

Heats of Formation. The energetic components for predicting the total molecular dissociation energies are given in Table 1. The electronic states and symmetry labels are included in Tables 1 and 2. The core−valence corrections are positive and range from 1.12 [$HB(NH_3)$] to 3.02 [$(CH_3)H_2B{-}NH_3$] kcal/mol. The scalar relativistic corrections are all negative and range from −0.23 [$HBCH_2$] to −0.61 [$(CH_3)H_2N{-}BH_3$] kcal/mol. We estimate that the error bars for the calculated heats of formation are ±1.0 kcal/mol, considering errors in the energy extrapolation, frequencies, and other electronic energy components. The largest error is most likely in the valence contribution and extrapolation to the complete basis set limit followed by the prediction of the zero-point energy. An estimate of the potential for significant multireference character in the wave function can be obtained from the T_1 diagnostic[60] for the CCSD calculation. The values for the T_1 diagnostics are small (<0.03), showing that the wave functions are dominated by a single configuration. The T_1 diagnostics are given as Supporting Information (Table SI-7).

The calculated CCSD(T)/CBS heats of formation for the molecules are given in Table 2 and compared to experimental data where available.[61−65] In general, the heats of formation calculated at the G3(MP2) level are within 2 kcal/mol of the more accurate CCSD(T) value, except for $H_3B{-}NH_3$, where the difference is predicted to be 2.9 kcal/mol. The heats of formation of the methyl amines are known from experiment. The CCSD(T)/CBS value for CH_3NH_2 is within 1 kcal/mol of experiment, as expected. The heats of formation of $(CH_3)_2NH$ and $(CH_3)_3N$ were calculated at the G3(MP2) level using isodesmic reaction schemes. The G3(MP2) isodesmic values are similar to the G3(MP2) values calculated from the atomization energies. The differences of the calculated values for the amines from experiment are less than 2 kcal/mol, and the calculated values are less negative than the experimental values. The calculated values for $B(CH_3)_3$, $B(CH_3)_3NH_3$, and $N(CH_3)_3BH_3$ are in reasonable agreement with the experimental values.[62,64,65]

Dehydrogenation Reaction Energies. We can predict the heats of reaction for the dehydrogenation of *N*-methylammonia borane and ammonia *B*-methylborane (Table 3), and we use the CCSD(T) values at 298 K in our discussions below unless specified otherwise. The dehydrogenation of *N*-methylammonia borane can occur via two possible pathways. One is the removal of H_2 from across the B−N bond, resulting in the formation of $(CH_3)HN{=}BH_2$. This pathway is exothermic by −3.5 and −5.2 (G3(MP2)) kcal/mol, showing reasonable agreement of the G3(MP2) value with the more accurate CCSD(T) result. This value can be compared to the dehydrogenation of ammonia borane of $\Delta H = -5.1$ kcal/mol.[10] The effect of the methyl substituent at N is to decrease the exothermicity of the dehydrogenation reaction by 1.6 kcal/mol, making the reaction closer to thermonuetral. Dehydrogenation of *N*-methylammonia borane can also occur by the removal of H_2 from across C−N bond leading to the formation of a C=N double bond in $(BH_3)HN{=}CH_2$. This reaction is predicted to be endothermic by 28.0 and 26.3 (G3(MP2)) kcal/mol. This value is ~1 kcal/mol more endothermic than the dehydrogenation of $(CH_3)NH_2$ to give $H_2C{=}NH$ of 26.7 kcal/mol. Substitution of the $-BH_3$ group has a minimal effect on the dehydrogenation reaction across the C−N bond. This value can also be compared to the experimental value[48,66] of 32.6 kcal/mol for the dehydrogenation of C_2H_6. The latter pathway for the dehydrogenation process is unlikely due to its large endothermicity.

The dehydrogenation of ammonia *B*-methylborane can also occur via two pathways. Dehydrogenation across the B−N bond leads to the product $(CH_3)HB{=}NH_2$; this reaction is predicted to be exothermic by −9.4 and −11.0 (G3(MP2)) kcal/mol, again showing reasonable agreement of the G3(MP2) value with the more accurate CCSD(T) value. The dehydrogenation reaction at the B−N bond is more exothermic for methyl substitution on B as compared to that for methyl substitution on N. Dehydrogenation across the B−C bond leads to $(NH_3)HB{=}CH_2$, and this reaction is endothermic by 38.3 and 36.3 (G3(MP2)) kcal/mol. This value is ~6 kcal/mol less than the dehydrogenation enthalpy of $(CH_3)BH_2$ to give $H_2C{=}BH$ of 44.5 kcal/mol. This value is ~12 kcal/mol more endothermic than the dehydrogenation of C_2H_6.[48,66]

We predicted the heats of formation of *N*-dimethylammonia borane and ammonia *B*-dimethylborane, their thermodynamically favorable dehydrogenated derivatives, $(CH_3)_2N{=}BH_2$ and $(CH_3)_2B{=}NH_2$, and *N*-trimethylammonia borane and ammonia *B*-trimethylborane on the basis of isodesmic reactions at the G3(MP2) level (Table SI-6, Supporting Information). The calculated heats of formation at 0 and 298 K are given in Table 2. Although the dehydrogenation of *N*-dimethylammonia borane can occur via two possible pathways, we have chosen to focus only on the removal of H_2 from across the B−N bond, as the dehydrogenation reaction across the N−C bond is substantially endothermic. The dehydrogenation pathway forming $(CH_3)_2N{=}BH_2$ is predicted to be exothermic by only −1.8 (isodesmic G3(MP2)) and −3.6 (standard G3(MP2)) kcal/mol. The ad-

TABLE 2: Calculated Heats of Formation in kcal/mol (Experimental Values at 298 K in Parentheses)

	CCSD(T) unless noted		G3(MP2)	
molecule	theory (0 K)	theory (298 K)	theory (0 K)	theory (298 K)
$HBCH_2$ (C_{2v}−$^1A_1$)	53.2	52.4	54.1	53.2
$HBNH_2$ (C_s−$^2A'$)	36.2	34.4	37.8	36.1
$HNBH_2$ (C_1−^2A)	43.3	42.1	44.8	43.5
$HNCH_2$ (C_s−$^1A'$)	23.6	21.7	23.2	21.3
$HBCH_3$ (C_1−^2A)	61.4	59.8	62.3	60.9
$HBNH_3$ (C_1−^1A)	82.7	80.4	83.1	81.2
$HBNH_3$ (C_s−$^3A''$)	90.3	87.9	92.1	89.7
$HNBH_3$ (C_1−^3A)	83.4	81.3	85.0	82.7
$HNCH_3$ (C_s−$^2A''$)	45.9	43.3	45.9	43.3
H_2BCH_3 (C_s−$^1A'$)	10.3	7.7	11.6	9.1
H_2NCH_3 (C_s−$^1A'$)	−1.4[a]	−4.7[a] (−5.6 ± 0.2[b])	−0.5	−4.1
$H_2B{=}NH_2$ (C_{2v}−$^1A_1$)	−17.0[c]	−19.7[c]	−15.1	−17.8
$(CH_3)HB{=}NH_2$ (C_s−$^1A'$)	−30.5	−34.7	−29.2	−33.3
$(NH_3)HB{=}CH_2$ (C_s−$^1A'$)	17.2	13.0	18.1	14.0
$(CH_3)HN{=}BH_2$ (C_s−$^1A'$)	−12.8	−17.1	−11.4	−15.7
$(BH_3)HN{=}CH_2$ (C_s−$^1A'$)	18.7	14.4	20.1	15.9
$H_3B{-}NH_3$ (C_{3v}−$^1A_1$)	−10.2[c]	−14.6[c]	−7.4	−11.7
$(CH_3)H_2B{-}NH_3$ (C_s−$^1A'$)	−19.4	−25.3	−17.8	−23.5
$(CH_3)H_2N{-}BH_3$ (C_s−$^1A'$)	−7.6	−13.7	−5.7	−11.6
$B(CH_3)_2$ (C_2−^2A)	45.8[d]	42.6[d]	46.4	43.5
$HB(CH_3)_2$ (C_2−^1A)	−5.2[d]	−9.2[d]	−4.3	−8.1
$N(CH_3)_2$ (C_{2v}−$^1A_1$)	43.6[d]	39.9[d]	43.1	39.1
$HN(CH_3)_2$ (C_s−$^1A'$)	1.8[d]	−2.8[c] (−4.5 ± 0.4[b])	2.3	−2.9
$(CH_3)_2B{=}NH_2$ (C_{2v}−$^1A_1$)	−44.4[d]	−49.8[d]	−43.4	−48.6
$(CH_3)_2HB{-}NH_3$ (C_s−$^1A'$)	−30.9[d]	−38.1[d]	−29.5	−36.5
$(CH_3)_2N = BH_2$ (C_{2v}−$^1A_1$)	−11.3[d]	−16.9[d]	−10.4	−16.2
$(CH_3)_2HN{-}BH_3$ (C_s−$^1A'$)	−7.8[d]	−15.1[d]	−6.3	−13.8
$B(CH_3)_3$ (C_1−^1A)	−20.6[d]	−25.79[d] (−29.7,[e] −29.2 ± 3.0[f])	−20.0	−24.8
$N(CH_3)_3$ (C_{3v}−$^1A_1$)	1.5[d]	−4.4[d] (−5.6 ± 0.3[b])	1.5	−5.2
$(CH_3)_3B{-}NH_3$ (C_{3v}−$^1A_1$)	−43.0[d]	−51.5[d] (−54.1[e])	−42.0	−50.2
$(CH_3)_3N{-}BH_3$ (C_{3v}−$^1A_1$)	−9.2[d]	−17.8[d] (−20.3,[e] −20.4 ± 0.6[f])	−8.0	−17.2

[a] Reference 35c. [b] Reference 61. [c] Reference 10. Corrected for the new heat of formation of the B atom. [d] Calculated based on isodesmic reactions at the G3(MP2) level. [e] Reference 62. [f] Reference 64.

TABLE 3: Dehydrogenation Reactions (kcal/mol)

	CCSD(T)		G3(MP2)	
reaction	(0 K)	(298 K)	(0 K)	(298 K)
$H_3B{-}NH_3 \rightarrow H_2B{=}NH_2 + H_2$	−6.8[a]	−5.1[a]	−8.9	−7.3
$(CH_3)H_2N{-}BH_3 \rightarrow (CH_3)HN{=}BH_2 + H_2$	−5.2	−3.5	−6.9	−5.2
$(CH_3)H_2N{-}BH_3 \rightarrow (BH_3)HN{=}CH_2 + H_2$	26.3	28.0	24.5	26.3
$(CH_3)H_2B{-}NH_3 \rightarrow (CH_3)HB{=}NH_2 + H_2$	−11.1	−9.4	−12.6	−11.0
$(CH_3)H_2B{-}NH_3 \rightarrow (NH_3)HB{=}CH_2 + H_2$	36.6	38.3	34.7	36.3
$(CH_3)_2HN{-}BH_3 \rightarrow (CH_3)_2N{=}BH_2 + H_2$	−3.5	−1.8	−5.3	−3.6
$(CH_3)_2HB{-}NH_3 \rightarrow (CH_3)_2B{=}NH_2 + H_2$	−13.5	−11.7	−15.1	−13.3

[a] Reference 10.

ditional methyl substituent further decreases the exothermicity of the dehydrogenation reaction by 1.7 kcal/mol and becomes even closer to thermoneutral.

Similarly, we consider dehydrogenation of ammonia *B*-dimethylborane across the B−N bond as the dehydrogenation across the B−C bond is highly endothermic. The dehydrogenation pathway forming $(CH_3)_2B{=}NH_2$ is calculated to be −11.7 (isodesmic G3(MP2)) and −13.3 (standard G3(MP2)) kcal/mol. The second methyl substituent further increases the exothermicity by 2.3 kcal/mol compared to its monomethyl analogue and by 6.6 kcal/mol compared to ammonia borane, leading to a more exothermic dehydrogenation reaction.

Bond Energies. We first examine the effect of sequentially methylating ammonia borane at both B and N on the B−N dative σ-bond energy (Table 7) and use the values calculated at 0 K in our discussion below. Monomethylation of ammonia borane at N leads to a predicted 5.6 kcal/mol increase in the B−N dative σ-bond energy compared to that of ammonia borane.[10] The substitution of the second methyl group to form *N*-dimethylammonia borane leads to an additional 3.4 kcal/mol increase in the B−N dative σ-bond energy compared to that of the monomethyl analogue and a 9.0 kcal/mol increase compared to that of ammonia borane.[10] The B−N dative σ-bond energy of $(CH_3)_3N{-}BH_3$ shows a smaller increase of 1.1 kcal/mol compared to that of the dimethyl-substituted analogue and a total 10.1 kcal/mol increase compared to that of ammonia borane.[10] The calculated values for the B−N dative bond energies for methyl substitution at N can be compared to experimental estimates[67,68] at 298 K, as shown in Table 7. The largest difference was found for BH_3NH_3 where Haaland[67] estimated the value. We note that the calculations predict that methylation at N increases the B−N bond energy in contrast to Haaland's experimental prediction of an increase through dimethylation and a decrease for trimethylation. If one uses more modern values[62,64] for $\Delta H_f(N(CH_3)_3)$ and $\Delta H_f(N(CH_3)_3BH_3)$ and our best calculated value for BH_3, one obtains a value of 39.2 kcal/mol for the B−N dative bond energy for $N(CH_3)_3BH_3$, which is completely consistent with the predicted trends. In contrast, methylation of ammonia borane at B is predicted to have the opposite effect, and the B−N dative σ-bond energy of $(CH_3)_{(3-n)}H_nB{-}NH_3$ for $n = 2$, 1, and 0 are predicted to be 5.8, 9.9, and 13.1 kcal/mol less than that in $H_3B{-}NH_3$, respectively (Table 7). The calculated value for the B−N dative bond in $NH_3B(CH_3)_3$ can be compared with the experimental value[67,69] of 13.8 kcal/mol, and good agreement is found.

Our calculated dative bond energies can be compared with previous theoretical calculations. The G2(MP2) B−N dative bond energies at 0 K are in good agreement with our values,

TABLE 4: Calculated Imaginary Vibrational Frequencies (cm^{-1}) at the MP2/VTZ Level

molecule	symmetry	calculated	type
$H_2B=NH_2$ rot ($C_s-{}^1A'$)[a]	a″	778.9*i*	NH_2 rotation
$H_2B=NH_2$ rot−planar ($C_{2v}-{}^1A_1$)[a]	a_2	1186.2*i*	NH_2 rotation
	b_2	631.5*i*	N inversion
$(CH_3)HN=BH_2$ rot ($C_s-{}^1A'$)	a″	1028.4*i*	BH_2 rotation + NH wag
	a″	374.3*i*	NH wag + BH_2 rotation
	a″	71.9*i*	CH_3 rotation
$(BH_3)HN=CH_2$ rot ($C_s-{}^3A''$)	a″	192.0*i*	BH_3 rotation
$(CH_3)HB=NH_2$ rot ($C_s-{}^1A'$)	a″	601.5*i*	NH_2 rotation
	a″	99.6*i*	CH_3 rotation
$(NH_3)HB=CH_2$ rot ($C_s-{}^3A''$)	a″	555.5*i*	BH wag
	a″	81.1*i*	NH_3 rotation
$(CH_3)_2N = BH_2$ rot ($C_s-{}^1A'$)	a″	497.2*i*	BH_2 rotation
$(CH_3)_2N = BH_2$ rot ($C_{2v}-{}^1A_1$)	a_2	858.7*i*	BH_2 rotation
	b_1	254.0*i*	N inversion
$(CH_3)_2B=NH_2$ rot ($C_s-{}^1A'$)	a″	545.6*i*	NH_2 rotation
	a″	155.0*i*	asymm. CH_3 rotation
	a″	115.4*i*	symm. CH_3 rotation
$(CH_3)_2B=NH_2$ rot ($C_{2v}-{}^1A_1$)	a_2	852.6*i*	NH_2 rotation
	b_2	623.1*i*	N inversion
	a_2	170.8*i*	asymm. CH_3 rotation
	b_1	145.3*i*	symm. CH_3 rotation

[a] Reference 22.

and the MP2/TZ2P values[70] are too large by 2−3 kcal/mol. The MP2(full)6-311++G** and MP2/6-311++G** values are in reasonable agreement with our values, but how the ZPE was included and the temperature of the results were not given.[29,32] Calculations at the HF/6-31G* level[71] using isodesmic reactions give methylated boron−nitrogen bond energies that are too large and methylated nitrogen−boron bond energies that are too small. The HF/6-31G* methylated boron−nitrogen bond energies do have the correct qualitative trend of decreasing bond energy with increasing degrees of methylation, but the HF/6-31G* level does not get the correct trend for an increase in the dative bond energy with methylation at N, and in fact, HF/6-31G* does not predict any real methylation effect.

We estimate the π- and σ-bond energies of the various "double" bonds following the procedures we recently used for the Group IIIA−Group VA $H_2A=XH_2$ compounds based on rotation barriers.[22] The molecular structures for the optimized ground state as well as the transition state for rotation about the A=X bond are shown in Figures SI-1 and SI-2 of the Supporting Information. For the B=N bond, the transition state lies on the singlet surface as a dative π-bond is being broken. For the C=N and B=C bonds, a covalent π-bond is broken; therefore, we estimate the rotation barrier by calculating the energy of the triplet rotated transition state. For the rotated structures, the unique imaginary frequencies associated with each molecule are given in Table 4. The π-bond energies can be estimated from the magnitude of the energies of the rotation barrier, and the values for the rotation barriers are presented in Table 5. The adiabatic rotation energy barrier was calculated as the energy difference between the equilibrium ground-state configuration and the transition-state structure of C_s symmetry for torsion by 90° about the central A=X bond. In addition, we also calculated an intrinsic π-bond energy, which is defined as the adiabatic bond energy plus the energy used to invert the N atom in the rotated transition-state structure or the $C_{2v} \rightarrow C_{2v}$ rotation energies. The rotation barrier calculated at the MP2/VTZ level should be an excellent estimate of the CCSD(T)/CBS value; as in BH_2NH_2, the adiabatic and intrinsic π-bond energies were within 0.2 kcal/mol of each other at the CCSD(T)/CBS and MP2/VTZ levels.

TABLE 5: Adiabatic Rotation Barriers (π-Bond Energies) at 0 K at the MP2/VTZ Level (kcal/mol)

molecule	rotation (G.S. → C_s)
$H_2B=NH_2$[a]	29.7 (29.9)
$(CH_3)HN=BH_2$	36.8
$(BH_3)HN=CH_2$	71.3
$(CH_3)HB=NH_2$	26.3
$(NH_3)HB=CH_2$	63.0
$(CH_3)_2N = BH_2$	32.8
$(CH_3)_2B=NH_2$	25.3

[a] The value in parentheses was calculated at the CCSD(T)/CBS level; ref 22.

The adiabatic rotation barriers of $(CH_3)HB=NH_2$ and $(CH_3)HN=BH_2$ are predicted to be 3.4 kcal/mol less and 7.1 kcal/mol more than that of $H_2B=NH_2$. The higher rotational barrier for $(CH_3)HN=BH_2$ can be rationalized in terms of the electron-donating ability of the methyl group at N, leading to further delocalization of the increased electron density toward the empty p orbital on B and a stronger dative π-bond. The adiabatic rotation barriers of $(NH_3)HB=CH_2$ and $(BH_3)HN=CH_2$ are much larger, consistent with the former two molecules having only a dative π-bond and the latter two molecules having a covalent π-bond. In comparison, the measured rotational barriers for systems substituted with three alkyls and a phenyl on either B or N, for example, $(CH_3)_2NB(R)Ph$ and $Ph(R)N-B(CH_3)_2$, are lower, ranging from 10 to 19 kcal/mol.[72] Such low barriers are consistent with expected steric interactions which destabilize the planar ground states along with stabilizing resonance effects with the phenyl ring in the transition structures. The adiabatic π-bond energies of $(NH_3)HB=CH_2$ and $(BH_3)HN=CH_2$ are predicted to be comparable to the π-bond strength of C_2H_4 of 65 kcal/mol.[24] Our calculated value for the rotation barrier of C_2H_4 is 65.8 kcal/mol.[73] Similarly, we predict the adiabatic rotation barriers $(CH_3)_2B=NH_2$ and $(CH_3)_2N=BH_2$ to be 1.0 and 4.0 kcal/mol less, respectively, than those of their monomethyl analogues.

We also calculated a rotation barrier defined as the energy difference between the ground-state and the rotated transition-state structure that is corrected for any pyramidalization that may have occurred upon rotation. For $H_2B=NH_2$, the rotational

TABLE 6: Adiabatic ($\sigma + \pi$) Total Dissociation Energies and Adiabatic σ-Bond Energies 0 K at the CCSD(T) Level (kcal/mol)[a]

reaction	bond type	total dissociation energy	σ-bond energy
$H_2B{=}NH_2$ ($^1A_1$) → BH_2 ($^2A_1$) + $\cdot NH_2$ ($^2B_1$)	B=N	139.7[b]	109.8[b]
$(CH_3)HN{=}BH_2$ ($^1A'$) → BH_2 ($^2A_1$) + $H\cdot N\text{-}CH_3$ ($^2A''$)	B=N	136.1	99.3
$(BH_3)HN{=}CH_2$ ($^1A'$) → $:CH_2$ ($^3B_1$) + $HN{-}BH_3$ (^3A)	N=C	158.2	86.9
$(CH_3)HB{=}NH_2$ ($^1A'$) → NH_2 ($^2B_1$) + $H\cdot B\text{-}CH_3$ (^2A)	B=N	137.2	110.9
$(NH_3)HB{=}CH_2$ ($^1A'$) → $:CH_2$ ($^3B_1$) + $HB{-}NH_3$ (^1A)	B=C	158.9	95.9
$(CH_3)_2N{=}BH_2$ ($^1A_1$) → BH_2 ($^2A_1$) + $N(CH_3)_2$ ($^2A_1$)	B=N	132.3	99.5
$(CH_3)_2B{=}NH_2$ ($^1A_1$) → NH_2 ($^2B_1$) + $B(CH_3)_2$ (^2A)	B=N	135.4	110.1

[a] ΔH_f (BH_2) = 78.5 kcal/mol,[22] ΔH_f (NH_2) = 45.3 kcal/mol,[77] and ΔH_f (CH_2) = 93.5 kcal/mol.[77] [b] Reference 22.

TABLE 7: Adiabatic σ-Bond Energies (B.E.) in kcal/mol[a]

reaction	bond type	B.E. calc (0 K)	B.E. calc (298 K)	B.E. expt (298 K)	B.E. calc (0 or 298 K)[b]
$H_3B{-}NH_3$ ($^1A_1$) → BH_3 ($^1A_1'$) + $:NH_3$ ($^1A_1$)	B−N dative	25.9[c]	27.7	31.1 ± 1.0[d]	26.0 G2(MP2)[e] 28.3 MP2/TZ2P[f] (28.5) MP4[g] 27.9 MP2[h] 26.5 MP2[i] 29.6 MP2[m]
$(CH_3)HN{=}BH_2$ ($^1A'$) → $\cdot CH_3$ ($^2A_2''$) + $H\cdot N{=}BH_2$ (^2A)	C−N covalent	91.7	94.2		
$(BH_3)HN{=}CH_2$ ($^1A'$) → BH_3 ($^1A_1'$) + $H{:}N{=}CH_2$ ($^1A'$)	B−N dative	30.2	31.7		
$(CH_3)HB{=}NH_2$ ($^1A'$) → $\cdot CH_3$ ($^2A_2''$) + $H\cdot B{=}NH_2$ ($^2A'$)	B−C covalent	102.4	104.1		
$(NH_3)HB{=}CH_2$ ($^1A'$) → $:NH_3$ ($^1A_1$) + $HB{=}CH_2$ ($^1A_1$)	B−N dative	26.4	28.1		
$(CH_3)H_2N{-}BH_3$ ($^1A'$) → BH_3 ($^1A_1'$) + $NH_2(CH_3)$ ($^1A'$)	B−N dative	31.5	33.4	35.0 ± 0.8[d]	31.9 G2(MP2)[e] (31.3) HF/6-31G*[g] 33.1 MP2[h] 32.3 MP2[i] 34.7 MP2[m]
$(CH_3)H_2B{-}NH_3$ ($^1A'$) → $BH_2(CH_3)$ ($^1A'$) + $:NH_3$ ($^1A_1$)	B−N dative	20.1	21.7		(23.5) HF/6-31G*[g]
$(CH_3)_2HN{-}BH_3$ ($^1A'$) → BH_3 ($^1A_1'$) + $HN(CH_3)_2$ ($^1A'$)	B−N dative	34.9	36.7	36.4 ± 1.0[d]	35.2 G2(MP2)[e] (31.8) HF/6-31G*[g] 35.9 MP2[h] 35.6 MP2[i] 37.3 MP2[m]
$(CH_3)_2HB{-}NH_3$ ($^1A'$) → $HB(CH_3)_2$ (^1A) + $:NH_3$ ($^1A_1$)	B−N dative	16.0	17.6		(19.0) HF/6-31G*[g]
$(CH_3)_3N{-}BH_3$ ($^1A_1$) → BH_3 ($^1A_1'$) + $N(CH_3)_3$ ($^1A_1$)	B−N dative	36.0	37.8	34.8 ± 0.5[d] 39.2[j] 31.5[k]	36.2 G2(MP2)[e] 38.7 MP2/TZ2P[g] (30.6) HF/6-31G*[g] 36.6 MP2[h] 36.8 MP2[i]
$(CH_3)_3B{-}NH_3$ ($^1A_1$) → $B(CH_3)_3$ ($^1A_1'$) + $:NH_3$ ($^1A_1$)	B−N dative	12.8	14.5	13.8 ± 0.3[l]	(14.9) HF/6-31G*[g] 15.4 MP2[i]

[a] ΔH_f (BH_3) = 25.3 ± 0.7 kcal/mol[10] recalculated with the new heat of formation of B of 135.1 ± 0.2 kcal/mol,[49] ΔH_f (CH_3) = 35.7 kcal/mol,[77] and ΔH_f (NH_3) = −9.6 ± 0.5 kcal/mol,[10] all at 0 K. The 298 K values are ΔH_f (BH_3) = 24.4, ΔH_f (NH_3) = −11.3, and ΔH_f (CH_3) = 35.0 kcal/mol. [b] Values in parentheses at 298 K. [c] Reference 10. [d] Reference 67. [e] References 30 and 31. [f] Reference 70. [g] Reference 71. [h] Reference 29 MP2(full)/6-311++G**. [i] Reference 32 MP2/6-311++G**. [j] Re-evaluated from literature. See text. [k] Reference 68. [l] References 67 and 69. [m] Reference 33, MP2/6-311G** at 0 K with ZPE included.

barrier difference is 4.0 kcal/mol (3.9 kcal/mol at the CCSD(T)/CBS level) due to the inversion barrier of the $-NH_2$ moiety in the rotated structure. Similarly for $(CH_3)_2N{=}BH_2$ and $(CH_3)_2B{=}NH_2$, we predict an intrinsic π-bond strength of 38.1 and 29.1 kcal/mol, a difference of 5.3 and 3.8 kcal/mol due to the inversion barrier at N. The inversion barriers in methyl-substituted amines have been previously calculated using the approximate PRDDO method and ab inito levels employing a DZP basis set giving barriers of 4.7, 5.1, 5.4, and 9.6 kcal/mol for NH_3, CH_3NH_2, $(CH_3)_2NH$, and $(CH_3)_3N$, respectively.[74] The inversion barrier of $(CH_3)_2N{=}BH_2$ is essentially the same as that of $(CH_3)_2NH$, indicating no substituent effect of the $=BH_2$ group. Similarly, the inversion barriers of $(CH_3)_2B{=}NH_2$ and $H_2B{=}NH_2$ are essentially the same, indicating no effect of the $-CH_3$ groups on the inversion barrier at N, indicating that inversion is not as important as delocalization. The orbital diagrams (obtained at the density functional theory B3LYP/DZVP2 level;[75,76] see Supporting Information) are consistent with these effects.

The adiabatic BDEs (Tables 6 and 7) correspond to the sum of the σ- and π-bond energies (doubly bonded compounds) or to the σ-bond energies (singly bonded compounds). The C−N adiabatic BDE of $(CH_3)HN{=}BH_2$ is equal to the diabatic BDE as the ground state of the separated species can be directly derived from the bonding configuration in the molecule. The C−N adiabatic BDE (value of $\Delta H_f(CH_3)$ from ref 77) can be compared to the value of 82.4 kcal/mol in $H_3C{-}NH_2$, showing a substituent effect of 9.3 kcal/mol for the $-BH_2$ group. The B=N adiabatic BDE of $(CH_3)HN{=}BH_2$ is 3.6 kcal/mol less than the adiabatic ($\sigma + \pi$) total dissociation energy of $H_2B{=}NH_2$,[22] showing a small effect of the methyl substituent on the B=N BDE. This value is substantially less than the C=C BDE in ethylene of 171.0 kcal/mol.[23]

We consider the B−N and N=C BDEs of $(BH_3)HN{=}CH_2$, the dehydrogenated product of *N*-methylammonia borane from dehydrogenation across the N−C bond, that has a dative B−N bond. The $=CH_2$ group increases the B−N dative BDE by 4.3 kcal/mol as compared to the B−N donor σ-bond in $H_3B{-}NH_3$.[10]

The N$=$C bond dissociates to ground state $^3B_1$ CH_2 and ^3A $HN-BH_3$, so the adiabatic and diabatic BDEs are the same. This BDE is comparable to the C$=$N adiabatic BDE in $H_2C=NH$ of 155.5 kcal/mol, showing a minimal substitution effect of 2.7 kcal/mol for the $-BH_3$ group on the C$=$N diabatic BDE. This value is about 13 kcal/mol less than the C$=$C BDE in ethylene.[23]

The B$-$C adiabatic BDE in $(CH_3)HB=NH_2$ (Table 7) is about the same as the B$-$C adiabatic BDE in H_3C-BH_2 of 102.2 kcal/mol, showing no substituent effect for the $=NH_2$ group. The B$=$N adiabatic BDE is slightly less than the adiabatic ($\sigma + \pi$) BDE in $H_2B=NH_2$,[22] showing a minimal substituent effect for the $-CH_3$ group. It is also slightly higher by ~1 kcal/mol than the B$=$N BDE in $(CH_3)HN=BH_2$.

The B$-$N dative BDE in $(NH_3)HB=CH_2$ is approximately equal to the B$-$N donor σ-bond in H_3B-NH_3[10] and is ~4 kcal/mol less than that in $(BH_3)HN=CH_2$. The B$=$C adiabatic BDE can be compared to that in $H_2C=BH$ of 145.0 kcal/mol, showing a 13.9 kcal/mol substituent effect of the $-NH_3$ group. We can define a diabatic B$=$C BDE with dissociation occurring to the excited triplet state of $HB-NH_3$ and the $^3B_1$ ground state of CH_2 that more closely represents the bonding electron configuration in the molecule. The diabatic B$=$C BDE in $(NH_3)HB=CH_2$ is 166.6 kcal/mol. The analogous diabatic BDE in $H_2C=BH$, in which dissociation occurs to the excited $^3\Pi$ state of BH, is 174.6 kcal/mol, 8.0 kcal/mol higher than the B$=$C diabatic BDE in $(NH_3)HB=CH_2$. (The experimental singlet$-$triplet splitting of the BH radical is 10410 cm^{-1} (29.7 kcal/mol).[78]) The diabatic BDE in $H_2C=BH$ is 3.6 kcal/mol higher than the C$=$C BDE in ethylene.[23]

For the dimethyl-substituted compounds, the B$=$N adiabatic BDEs in $(CH_3)_2N=BH_2$ and $(CH_3)_2B=NH_2$ are 7.4 and 4.3 kcal/mol less, respectively, than that in $H_2B=NH_2$,[22] consistent with an approximately additive methyl substituent effect as these BDEs are less than those of their respective monomethyl analogues by 3.8 and 1.8 kcal/mol.

The adiabatic σ-bond energies of the doubly bonded molecules are calculated as the difference between the adiabatic BDE of the optimized ground-state structure, representing the sum of the ($\sigma + \pi$) bond energies, and the corresponding adiabatic rotational energy barrier, representing the π-bond energy. The adiabatic σ-bond strengths for $(CH_3)HN=BH_2$, $(BH_3)HN=CH_2$, $(CH_3)HB=NH_2$, $(NH_3)HB=CH_2$, $(CH_3)_2N=BH_2$, and $(CH_3)_2B=NH_2$ from the ($\sigma + \pi$) adiabatic asymptote using the adiabatic rotation barriers are given in Table 5. The adiabatic σ-bond strengths for $(CH_3)HN=BH_2$, $(CH_3)HB=NH_2$, $(CH_3)_2N=BH_2$, and $(CH_3)_2B=NH_2$ can be compared to the adiabatic B$-$N σ-bond strength of 109.8 kcal/mol in $H_2B=NH_2$.[22] Comparing the adiabatic σ-bond strengths for $(CH_3)HN=BH_2$ versus $(CH_3)_2N=BH_2$ and $(CH_3)HB=NH_2$ versus $(CH_3)_2B=NH_2$, we note that sequential methylation essentially has no effect on the B$-$N σ-bond to within 1 kcal/mol (Table 6). The adiabatic B$-$N σ-bond strengths for $(CH_3)HB=NH_2$ and $(CH_3)_2B=NH_2$ are also comparable to the adiabatic C$-$C σ-bond strength in C_2H_4 of 106 kcal/mol based on the experimentally determined π-bond strength of 65 kcal/mol[24] as well as the calculated value[73] of 65.8 kcal/mol and the adiabatic C$=$C BDE.[23] The fact that they are slightly more stable is consistent with the fact that the bonds in $(CH_3)HB=NH_2$ and $(CH_3)_2B=NH_2$ include some ionic character. The adiabatic B$-$C σ-bond strength of $(NH_3)HB=CH_2$ is slightly less endothermic by an average of 6.2 kcal/mol compared to those in H_3C-BH_2 and $(CH_3)HB=NH_2$ of 102.2 and 102.0 kcal/mol, respectively. The adiabatic N$-$C σ-bond strength of $(BH_3)HN=CH_2$ compares well with the adiabatic N$-$C σ-bond strengths in H_3C-NH_2 and $(CH_3)HN=BH_2$ of 82.4 and 91.4 kcal/mol, respectively, being slightly more and slightly less endothermic by 4.5 kcal/mol, respectively.

TABLE 8: Calculated G3(MP2) Heats of Formation (kcal/mol)

molecule	theory (0 K)	theory (298 K)
c-$B_2N_2H_4$ (D_{2h})	−23.6	−27.1
c-$B_2N_2H_8$ (D_{2h})[a]	−43.9	−50.9
c-$B_3N_3H_6$ (D_{3h})[a]	−106.5	−112.4
c-$B_3N_3H_{12}$ twist-boat (C_3)[a]	−82.6	−93.5
c-$B_4N_4H_8$ (D_{4h})	−123.3	−131.0
c-$B_4N_4H_{16}$ (C_{4v})	−95.2	−110.0
c-$B_2N_2H_2(CH_3)_2$ trans (C_i)	−16.1	−21.6
c-$B_2N_2H_6(CH_3)_2$ trans (C_{2h})	−40.2	−50.0
c-$B_3N_3H_3(CH_3)_3$ (C_{3h})	−94.2	−103.5
c-$B_3N_3H_9(CH_3)_3$ (C_{3v})	−78.4	−93.6
c-$B_4N_4H_4(CH_3)_4$ (S_4)	−99.4	−111.8
c-$B_4N_4H_{12}(CH_3)_4$ (C_1)	−99.2	−119.6
$(H_3BH_2N)H_2C-CH_2(NH_2BH_3)$ (C_s)	0.3	−10.5
$(H_2B=NH)H_2C-CH_2(NH_2BH_3)$ (C_1)	−7.6	−16.8
$(H_3B)HN=CH-CH_2(NH_2BH_3)$ (C_1)	24.3	17.4
$(H_3BH_2N)HC=CH(NH_2BH_3)$ (C_i)	30.4	21.5
$(H_2B=NH)H_2C-CH_2(HN=BH_2)$ (C_i)	−14.8	−22.4
$(H_3B)HN=CHHC=NH(BH_3)$ (C_{2h})	47.2	40.0
$(H_3BH_2N)C\equiv C(NH_2BH_3)$ (C_2)	88.2	81.4
$(H_2B=NH)HC=CH(NH_2BH_3)$ (C_1)	20.6	13.2
$(H_2B=NH)HC=CH(HN=BH_2)$ (C_{2h})	7.3	1.4
$(H_3NH_2B)H_2C-CH_2(BH_2NH_3)$ (C_s)	−19.0	−29.3
$(H_2N=BH)H_2C-CH_2(BH_2NH_3)$ (C_1)	−30.8	−39.6
$(H_3N)HB=CH-CH_2(BH_2NH_3)$ (C_1)	16.6	7.9
$(H_3NH_2B)HC=CH(BH_2NH_3)$ (C_i)	2.0	−6.6
$(H_2N=BH)H_2C-CH_2(HB=NH_2)$ (C_i)	−41.4	−48.6
$(H_3N)HB=CH-HC=BH(NH_3)$ (C_{2h})	47.8	40.7
$(H_3NH_2B)C\equiv C(BH_2NH_3)$ (C_2)	19.5	12.7
$(H_2N=BH)HC=CH(BH_2NH_3)$ (C_1)	−8.5	−15.7
$(H_2N=BH)HC=CH(HB=NH_2)$ (C_{2h})	−21.0	−26.6

[a] Taken from ref 11 and recalculated with new heat of formation of B of 135.1 ± 0.2 kcal/mol.[49]

Properties of Larger Compounds. The G3(MP2) method predicts reasonable BDEs and dehydrogenation energies; therefore, we can use this method for larger B$-$C$-$N compounds, which would be too computationally expensive to calculate at the CCSD(T) level. We have used the G3(MP2) method to predict the heats of formation (Table 8) and dehydrogenation energies (Table 9) of the methlyated cyclodi-, cyclotri-, and cyclotetraborazanes and use the 298 K values in our discussion below. The experimental heat of formation of the N-methylated c-$B_3N_3H_3(CH_3)_3$ compound has been reported to be -217 ± 1 kcal/mol, which is clearly incorrect.[63,79] The cis and *trans* isomers of *N*-dimethyl cyclodiborazane, c-$B_2N_2H_6(CH_3)_2$, are calculated to be the same at 298 K, slightly favoring the trans isomer at 0 K. Dehydrogenation of c-$B_2N_2H_6(CH_3)_2$ to give c-$B_2N_2H_2(CH_3)_2 + 2H_2$ is calculated to be 4.6 kcal/mol more endothermic than the equivalent nonmethylated reaction c-$B_2N_2H_8 \rightarrow c$-$B_2N_2H_4 + 2H_2$,[11] showing that methylation at N in the cyclodiborazane compound increases the endothermicity of the dehydrogenation reaction. Dehydrogenation of c-$B_3N_3H_9(CH_3)_3$ to give three H_2 molecules is calculated to be 12.4 kcal/mol less exothermic than the equivalent reaction of c-$B_3N_3H_{12}$ (twist-boat),[11] indicating a larger substituent effect of the $-CH_3$ groups on reducing the exothermicity of the dehydrogenation reaction. Dehydrogenation of c-$B_4N_4H_{12}(CH_3)_4$ to give c-$B_4N_4H_4(CH_3)_4 + 4H_2$ is calculated to be near-thermoneutral and 28.8 kcal/mol more endothermic than the equivalent nonmethylated cyclotetraborazane reaction c-$B_4N_4H_{16} \rightarrow c$-$B_4N_4H_8 + 4H_2$.

TABLE 9: Dehydrogenation Reactions at the G3(MP2) level (kcal/mol)

First Dehydrogenation Step	(0 K)	(298 K)
$c\text{-}B_2N_2H_8 \rightarrow c\text{-}B_2N_2H_4 + 2H_2$	17.9	21.6
$c\text{-}B_3N_3H_{12}$ twist-boat $\rightarrow c\text{-}B_3N_3H_6 + 3H_2$	−27.5[a]	−22.2[a]
$c\text{-}B_4N_4H_{16} \rightarrow c\text{-}B_4N_4H_8 + 4H_2$	−33.0	−25.4
$c\text{-}B_2N_2H_6(CH_3)_2 \rightarrow c\text{-}B_2N_2H_2(CH_3)_2 + 2H_2$	21.6	26.2
$c\text{-}B_3N_3H_9(CH_3)_3 \rightarrow c\text{-}B_3N_3H_3(CH_3)_3 + 3H_2$	−19.4	−13.0
$c\text{-}B_4N_4H_{12}(CH_3)_4 \rightarrow c\text{-}B_4N_4H_4(CH_3)_4 + 4H_2$	−7.3	3.4
$(H_3BH_2N)H_2C{-}CH_2(NH_2BH_3) \rightarrow (H_2B{=}NH)H_2C{-}CH_2(NH_2BH_3) + H_2$	−9.0	−7.4
$(H_3BH_2N)H_2C{-}CH_2(NH_2BH_3) \rightarrow (H_3B)HN{=}CH{-}CH_2(NH_2BH_3) + H_2$	22.9	26.7
$(H_3BH_2N)H_2C{-}CH_2(NH_2BH_3) \rightarrow (H_3BH_2N)HC{=}CH(NH_2BH_3) + H_2$	29.0	30.8
$(H_3NH_2B)H_2C{-}CH_2(BH_2NH_3) \rightarrow (H_2N{=}BH)H_2C{-}CH_2(BH_2NH_3) + H_2$	−13.0	−11.4
$(H_3NH_2B)H_2C{-}CH_2(BH_2NH_3) \rightarrow (H_3N)HB{=}CHC{-}H_2(BH_2NH_3) + H_2$	34.4	36.1
$(H_3NH_2B)H_2C{-}CH_2(BH_2NH_3) \rightarrow (H_3NH_2B)HC{=}CH(BH_2NH_3) + H_2$	19.8	21.6
Second Dehydrogenation Step		
$(H_2B{=}NH)H_2C{-}CH_2(NH_2BH_3) \rightarrow (H_2B{=}NH)H_2CCH_2(HN{=}BH_2) + H_2$	−8.4	−6.8
$(H_3B)HN{=}CH{-}CH_2(NH_2BH_3) \rightarrow (H_3B)HN{=}CHHC{=}NH(BH_3) + H_2$	21.7	21.5
$(H_3BH_2N)HC{=}CH(NH_2BH_3) \rightarrow (H_3BH_2N)C{\equiv}C(NH_2BH_3) + H_2$	56.6	58.8
$(H_2B{=}NH)H_2C{-}CH_2(NH_2BH_3) \rightarrow (H_2B{=}NH)HC{=}CH(NH_2BH_3) + H_2$	27.0	28.9
$(H_2N{=}BH)H_2C{-}CH_2(BH_2NH_3) \rightarrow (H_2N{=}BH)H_2C{-}CH_2(HB{=}NH_2) + H_2$	−11.8	−10.2
$(H_3N)HB{=}CH{-}CH_2(BH_2NH_3) \rightarrow (H_3N)HB{=}CH{-}HC{=}BH(NH_3) + H_2$	30.0	31.6
$(H_3NH_2B)HC{=}CH(BH_2NH_3) \rightarrow (H_3NH_2B)C{\equiv}C(BH_2NH_3) + H_2$	16.3	18.2
$(H_2N{=}BH)H_2C\text{-}CH_2(BH_2NH_3) \rightarrow (H_2N{=}BH)HC{=}CH(BH_2NH_3) + H_2$	21.0	22.7
Third Dehydrogenation Step		
$(H_2B{=}NH)H_2C{-}CH_2(HN{=}BH_2) \rightarrow (H_2B{=}NH)HC{=}CH(HN{=}BH_2) + H_2$	19.2	20.9
$(H_2N{=}BH)H_2C{-}CH_2(BH{=}NH_2) \rightarrow (H_2N{=}BH)HC{=}CH(HB{=}NH_2) + H_2$	20.9	22.6

[a] Taken from ref 11 and recalculated with new heat of formation of B of 135.1 ± 0.2 kcal/mol.[49]

We also studied the effect of substituting NH_2BH_3 and BH_2NH_3 for H in C_2H_6. Dehydrogenation of $(H_3BH_2N)H_2C{-}CH_2(NH_2BH_3)$ (**A**) and $(H_3NH_2B)H_2C{-}CH_2(BH_2NH_3)$ (**B**) can occur by several pathways. The most thermodynamically favorable pathway is dehydrogenation across the dative B−N bond with the first dehydrogenation step predicted to be 2.2 and 0.4 kcal/mol more exothermic than the equivalent dehydrogenation reactions of $(CH_3)H_2N{-}BH_3$ and $(CH_3)H_2B{-}NH_3$ of −5.2 and −11.0 kcal/mol, respectively. The other possible dehydrogenation pathways are predicted to be largely endothermic. The first dehydrogenation reaction across the C−N and B−C bonds yielding $(H_3B)HN{=}CH{-}CH_2(NH_2BH_3)$ and $(H_3N)HB{=}CH{-}CH_2(BH_2NH_3)$ are essentially the same (within 0.4 kcal/mol) as the equivalent dehydrogenation reaction of $(CH_3)H_2N{-}BH_3$ and $(CH_3)H_2B{-}NH_3$ of 26.3 and 36.3 kcal/mol, respectively. The dehydrogenation energies of **A** and **B** across the C−C bond are calculated to be 2 and 11 kcal/mol less endothermic, respectively, than the experimental value of 32.6 kcal/mol for the dehydrogenation of C_2H_6.[48,66] We obtain values of 32.8[34] and 30.8 kcal/mol for the equivalent reaction at the CCSD(T) and G3(MP2) levels, respectively. The second dehydrogenation step is most favorable across the second available B−N dative bond, and the resulting reaction energies are slightly less exothermic by 0.6 and 1.2 kcal/mol than the equivalent first dehydrogenation step, respectively. We also considered a third dehydrogenation step occurring across the C−C bond with the consequent energies for $(H_2B{=}NH)H_2C{-}CH_2(HN{=}BH_2)$ and $(H_2N{=}BH)H_2C{-}CH_2(HB{=}NH_2)$ predicted to be endothermic, indicating that this avenue for dehydrogenation is not likely unless one can couple the exothermicity of the loss of H_2 across the B−N bonds with that of the endothermicity of elimination across the C−C bond.

Conclusions

Ammonia borane and methylamine borane melt at 35−42 °C over a weight range of 20−50% of the former in the latter. The melt temperature of these mixtures is lower than that of the pure materials by up to 25 °C for methylamine borane and by up to 80−85 °C for ammonia borane. We have predicted the heats of formation of *N*-methylammonia borane and ammonia *B*-methylborane and their various dehydrogenated derivates, as well as various molecules involved in the bond-breaking processes, at the CCSD(T)/CBS level plus additional corrections. We considered the possibility of several dehydrogenation pathways and found that dehydrogenation across the B−N bond is more favorable as opposed to dehydrogenation across the B−C and C−N bonds. Dehydrogenation of *N*-methylammonia borane is exothermic by −3.5 kcal/mol at the CCSD(T) level at 298 K, whereas for ammonia *B*-methylborane, it was slightly more exothermic, −9.4 kcal/mol at the CCSD(T) level at 298 K. The effects of methyl substitution on the dehydrogenation of BH_3NH_3 were studied. Dehydrogenation of *N*-dimethylammonia borane is exothermic by −1.8 kcal/mol at the CCSD(T) level at 298 K, showing a decreased exothermicity of 3.3 kcal/mol compared to that of BH_3NH_3. Methyl substitution at N improves the thermodynamics as the dehydrogenation reactions are closer to thermoneutral. Dehydrogenation of ammonia *B*-dimethylborane is exothermic by −11.7 kcal/mol at the CCSD(T) level at 298 K, showing an increase in the exothermicity compared to that of ammonia borane. Methyl substitution at B leads to unfavorable thermodynamics as the dehydrogenation reactions move further away from thermoneutral. Methyl substitution at N in the cycloborazane rings increases the endothermicity of the dehydrogenation reactions, and for $c\text{-}B_4N_4H_{12}(CH_3)_4$, the thermodynamics for dehydrogenation reaction become favorable as it is near-thermoneutral. Dehydrogenation of $c\text{-}B_2N_2H_6(CH_3)_2$, $c\text{-}B_3N_3H_9(CH_3)_3$, and $c\text{-}B_4N_4H_{12}(CH_3)_4$ producing two, three, and four molecules of H_2 is 26.2, −13.0, and 3.4 kcal/mol at the G3(MP2) level at 298 K, respectively.

Acknowledgment. Funding was provided, in part, by the Department of Energy, Office of Energy Efficiency and Renewable Energy under the Hydrogen Storage Grand Challenge, Solicitation No. DE-PS36-03GO93013. This work was done as part of the Chemical Hydrogen Storage Center. D.A.D. is indebted to the Robert Ramsay Endowment of the University of Alabama. Part of this work was performed at the W. R. Wiley Environmental Molecular Sciences Laboratory, a national scientific user facility sponsored by DOE's Office of Biological and Environmental Research and located at Pacific Northwest National Laboratory, operated for the DOE by Battelle.

Supporting Information Available: Melt temperatures as a function of weight percent; calculated geometry parameters at the MP2/VTZ level; calculated MP2/VTZ frequencies and total CCSD(T) energies as a function of basis set; isodesmic reaction energies at the G3(MP2) level; T_1 diagnostics; HOMOs of $(CH_3)HN{=}BH_2$, $(CH_3)HB{=}NH_2$, $(CH_3)_2N{=}BH_2$, and $(CH_3)_2B{=}NH_2$ at the B3LYP/DZVP2 level; and HOMOs of $(BH_3)HN{=}CH_2$ and $(NH_3)HB{=}CH_2$ at the B3LYP/DZVP2 level. This material is available free of charge via the Internet at http://pubs.acs.org.

References and Notes

(1) Stephens, F. H.; Pons, V.; Baker, R. T. *Dalton Trans.* **2007**, 2613.

(2) Karkamkar, A. J.; Aardahl, C. L.; Autrey, T. *Mater. Matters* **2007**, *2*, 6.

(3) (a) Wolf, G.; van Miltenburg, R. A.; Wolf, U. *Thermochim. Acta* **1998**, *317*, 111. (b) Wolf, G.; Baumann, J.; Baitalow, F.; Hoffmann, F. P. *Thermochim. Acta* **2000**, *343*, 19. (c) Baitalow, F.; Baumann, J.; Wolf, G.; Jaenicke-Rlobler, K.; Leitner, G. *Thermochim. Acta* **2002**, *391*, 159.

(4) Parvanov, V. M.; Schenter, G. K.; Hess, N. J.; Daemen, L. L.; Hartl, A.; Stowe, A. C.; Camaioni, D. M.; Autrey, T. *Dalton Trans.* **2008**, 4514.

(5) Stowe, A. C.; Shaw, W. J.; Linehan, J. C.; Schmid, B.; Autrey, T. *Phys. Chem. Chem. Phys.* **2007**, *9*, 1831.

(6) Shaw, W. J.; Linehan, J. C.; Szymczak, N. K.; Heldebrant, D. J.; Yonker, C.; Camaioni, D. M.; Baker, R. T.; Autrey, T. *Angew. Chem., Int. Ed.* **2008**, *47*, 7493.

(7) Stephens, F. H.; Baker, R. T.; Matus, M. H.; Grant, D. J.; Dixon, D. A. *Angew Chem. Int. Ed.,* **2007**, *46*, 746.

(8) Pons, V.; Baker, R. T.; Szymczak, N. K.; Heldebrant, D. J.; Linehan, J. C.; Matus, M. H.; Grant, D. J.; Dixon, D. A. *Chem. Commun.* **2008**, 6597.

(9) Gutowska, A.; Li, L.; Shin, Y.; Wang, Ch.; Li, S.; Linehan, J.; Smith, R. S.; Kay, B.; Schmid, B.; Shaw, W.; Gutowski, M.; Autrey, T. *Angew. Chem., Int. Ed.* **2005**, *44*, 2.

(10) Gutowski, M.; Dixon, D. A. *J. Chem. Phys. A* **2005**, *109*, 5129.

(11) Matus, M. H.; Anderson, K. A.; Camaioni, D. M.; Autrey, S. T.; Dixon, D. A. *J. Phys. Chem. A* **2007**, *111*, 4411.

(12) Klooster, W. T.; Koetzle, T. F.; Siegbahn, P. E. M.; Richardson, T. B.; Crabtree, R. H. *J. Am. Chem. Soc.* **1999**, *121*, 6337.

(13) Morrison, C. A.; Siddick, M. M. *Angew. Chem., Int. Ed.* **2004**, *43*, 4780.

(14) Richarson, T. B.; de Gala, S.; Crabtree, R. H.; Siegbahn, P. E. M. *J. Am. Chem. Soc.* **1995**, *117*, 12875.

(15) (a) Geanangel, R. A.; Shore, S. G. *Prep. Inorg. React.* **1966**, *3*, 123. (b) Framery, E.; Vaultier, M. *Heteroatom Chem.* **2000**, *11*, 218. (c) See also: Lane, C. F. Ammonia-Borane and Related N−B-H Compounds and Materials: Safety Aspects, Properties and Applications. http://www1.eere.energy.gov/hydrogenandfuelcells/pdfs/nbh_h2_storage_survey.pdf (2005).

(16) (a) Lane, C.; Baker, S. "Applied Research on the Use of Amine-Borane Materials for Hydrogen Storage. *DOE Hydrogen Program Annual Merit Review*; Project ID # STP8; Department of Energy: Arlington, VA, May 2007; http://www.hydrogen.energy.gov/pdfs/review07/stp_8_lane.pdf. (b) Lane, C. F. *Safety Analysis and Applied Research on the Use of Borane-Amines for Hydrogen Storage*; DOE Hydrogen Program Annual Progress Report Contract No. DE-FC36-05GO15060; Department of Energy: Washington, DC, November 2007; http://www.hydrogen.energy.gov/pdfs/progress07/iv_b_5j_lane.pdf.

(17) Geanangel, R. A.; Shore, S. G. *Prep. Inorg. React.* **1966**, *3*, 123.

(18) Jaska, C. A.; Temple, K.; Lough, A. J.; Manners, I. *Chem. Commun.* **2001**, 962.

(19) Alton, E. R.; Brown, R. D.; Carter, J. C.; Taylor, R. C. *J. Am. Chem. Soc.* **1959**, *81*, 3550.

(20) Bartlett, R. J.; Musial, M. *Rev. Mod. Phys.* **2007**, *79*, 291.

(21) Sander, S. P.; Friedl, R. R.; Ravishankara, A. R.; Golden, D. M.; Kolb, C. E.; Kurylo, M. J.; Huie, R. E.; Orkin, V. L.; Molina, M. J.; Moortgat, G. K.; Finlayson-Pitts, B. J. *Chemical Kinetics and Photochemical Data for Use in Atmospheric Studies: Evaluation Number 14*; JPL Publication 02-25, National Aeronautics and Space Administration; Jet Propulsion Laboratory, California Institute of Technology: Pasadena, CA, 2003; http://jpldataeval.jpl.nasa.gov/pdf/JPL_02−25_rev02.pdf.

(22) Grant, D. J.; Dixon, D. A. *J. Phys. Chem. A* **2006**, *110*, 12955.

(23) Ervin, K. M.; Gronert, S.; Barlow, S. E.; Gilles, M. K.; Harrison, A. G.; Bierbaum, V. M.; DePuy, C. H.; Lineberger, W. C.; Ellison, G. B. *J. Am. Chem. Soc.* **1990**, *112*, 5750.

(24) Douglas, J. E.; Rabinovitch, B. S.; Looney, F. S. *J. Chem. Phys.* **1955**, *23*, 315.

(25) Bauer, S. H. *J. Am. Chem. Soc.* **1937**, *59*, 1823.

(26) Cassoux, P.; Kuczkowski, R. L.; Bryan, P. S.; Taylor, R. C. *Inorg. Chem.* **1975**, *14*, 126.

(27) Iijima, K.; Adachi, N.; Shibata, S. *Bull. Chem. Soc. Jpn.* **1984**, *57*, 3269.

(28) Bowden, M. E.; Brown, I. W. M.; Gainsford, G. J.; Wong, H. *Inorg. Chim. Acta* **2008**, *361*, 2147.

(29) Aldridge, S.; Downs, A. J.; Tang, C. Y.; Parsons, S.; Clarke, M. C.; Johnstone, R. D.; Robertson, H. E.; Rankin, D. W.; Wann, D. A. *J. Am. Chem. Soc.* **2009**, *131*, 2231.

(30) Anane, H.; Abdellah, J.; Boutalib, A.; Nebot-Gil, I.; Tomás, F. *J. Mol. Struct.: THEOCHEM* **1998**, *455*, 51.

(31) Anane, H.; Boutalib, A.; Nebot-Gil, I.; Tomás, F. *Chem. Phys. Lett.* **1998**, *287*, 575.

(32) Gilbert, T. M. *J. Phys. Chem. A* **2004**, *108*, 2550.

(33) Sun, C.-H.; Yao, Z.-D.; Du, A.-J.; Smith, S.; Lu, G.-Q. *Phys. Chem. Chem. Phys.* **2008**, *10*, 6104.

(34) (a) Feller, D.; Peterson, K. A. *J. Chem. Phys.* **1998**, *108*, 154. (b) Feller, D.; Peterson, K. A. *J. Chem. Phys.* **1999**, *110*, 8384. (c) Feller, D. *J. Chem. Phys.* **1999**, *111*, 4373. (d) Feller, D.; Sordo, J. A. *J. Chem. Phys.* **2000**, *113*, 485.

(35) (a) Feller, D.; Dixon, D. A. *J. Phys. Chem. A* **1999**, *103*, 6413. (b) Feller, D.; Dixon, D. A. *J. Phys. Chem. A* **2000**, *104*, 3048. (c) Feller, D.; Dixon, D. A. *J. Chem. Phys.* **2001**, *115*, 3484. (d) Dixon, D. A.; Feller, D. *J. Phys. Chem. A* **1998**, *102*, 8209. (e) Dixon, D. A.; Feller, D.; Sandrone, G. *J. Phys. Chem. A* **1999**, *103*, 4744. (f) Wagner, A. F.; Ruscic, B.; Harding, L. B.; Asher, R. L.; Feller, D.; Dixon, D. A.; Peterson, K. A.; Song, Y.; Ng, C.-Y.; Liu, J.; Chen, W.; Schwenke, D. W. *J. Phys. Chem. A* **2002**, *106*, 2727. (g) Dixon, D. A.; Feller, D.; Peterson, K. A. *J. Chem. Phys.* **2001**, *115*, 2576. (h) Dixon, D. A.; Feller, D.; Peterson, K. A. *J. Phys. Chem. A* **1998**, *102*, 7053. (i) Ruscic, B.; Wagner, A. F.; Harding, L. B.; Asher, R. L.; Feller, D.; Dixon, D. A.; Peterson, K. A.; Song, Y.; Qian, X.; Ng, C.-Y.; Liu, J.; Chem, W.; Schwenke, D. W. *J. Phys. Chem. A* **2002**, *106*, 2727. (j) Pollack, L.; Windus, T. L.; de Jong, W. A.; Dixon, D. A. *J. Phys. Chem. A* **2005**, *109*, 6934.

(36) (a) Dunning, T. H., Jr. *J. Chem. Phys.* **1989**, *90*, 1007. (b) Kendall, R. A.; Dunning, T. H., Jr.; Harrison, R. J. *J. Chem. Phys.* **1992**, *96*, 6796. (c) Woon, D. E.; Dunning, T. H., Jr. *J. Chem. Phys.* **1993**, *98*, 1358. (d) Dunning, T. H., Jr.; Peterson, K. A.; Wilson, A. K. *J. Chem. Phys.* **2001**, *114*, 9244. (e) Wilson, A. K.; Woon, D. E.; Peterson, K. A.; Dunning, T. H., Jr. *J. Chem. Phys.* **1999**, *110*, 7667.

(37) Amos, R. D.; Bernhardsson, A.; Berning, A.; Celani, P.; Cooper, D. L.; Deegan, M. J. O.; Dobbyn, A. J.; Eckert, F.; Hampel, C.; Hetzer, G.; Knowles, P. J.; Korona, T.; Lindh, R.; Lloyd, A. W.; McNicholas, S. J.; Manby, F. R.; Meyer, W.; Mura, M. E.; Nicklass, A.; Palmieri, P.; Pitzer, R.; Rauhut, G.; Schütz, M.; Schumann, U.; Stoll, H., Stone, A. J.; Tarroni, R.; Thorsteinsson, T.; Werner, H.-J. *MOLPRO: a Package of Ab Initio Programs*, version 2002.6; Universität Stuttgart: Stuttgart, Germany and University of Birmingham: Birmingham, U.K., 2002.

(38) Peterson, K. A.; Woon, D. E.; Dunning, T. H., Jr. *J. Chem. Phys.* **1994**, *100*, 7410.

(39) Peterson, K. A.; Dunning, T. H., Jr. *J. Chem. Phys.* **2002**, *117*, 10548.

(40) Moore, C. E. *Atomic Energy Levels As Derived from the Analysis of Optical Spectra, Volume 1, H to V*; U.S. National Bureau of Standards Circular 467; U.S. Department of Commerce, National Technical Information Service, COM-72-50282: Washington, DC, 1949.

(41) Davidson, E. R.; Ishikawa, Y.; Malli, G. L. *Chem. Phys. Lett.* **1981**, *84*, 226.

(42) (a) Douglas, M.; Kroll, N. M. *Ann. Phys.* **1974**, *82*, 89. (b) Hess, B. A. *Phys. Rev. A* **1985**, *32*, 756. (c) Hess, B. A. *Phys. Rev. A* **1986**, *33*, 3742.

(43) Pople, J. A.; Binkley, J. S.; Seeger, R. *Int. J. Quant. Chem., Quantum Chem. Symp.* **1976**, *10*, 1.

(44) Frisch, M. J.; Trucks, G. W.; Schlegel, H. B.; Scuseria, G. E.; Robb, M. A.; Cheeseman, J. R.; Montgomery, J. A., Jr.; Vreven, T.; Kudin, K. N.; Burant, J. C.; Millam, J. M.; Iyengar, S. S.; Tomasi, J.; Barone, V.; Mennucci, B.; Cossi, M.; Scalmani, G.; Rega, N.; Petersson, G. A.; Nakatsuji, H.; Hada, M.; Ehara, M.; Toyota, K.; Fukuda, R.; Hasegawa, J.; Ishida, M.; Nakajima, T.; Honda, Y.; Kitao, O.; Nakai, H.; Klene, M.; Li,

X.; Knox, J. E.; Hratchian, H. P.; Cross, J. B.; Bakken, V.; Adamo, C.; Jaramillo, J.; Gomperts, R.; Stratmann, R. E.; Yazyev, O.; Austin, A. J.; Cammi, R.; Pomelli, C.; Ochterski, J. W.; Ayala, P. Y.; Morokuma, K.; Voth, G. A.; Salvador, P.; Dannenberg, J. J.; Zakrzewski, V. G.; Dapprich, S.; Daniels, A. D.; Strain, M. C.; Farkas, O.; Malick, D. K.; Rabuck, A. D.; Raghavachari, K.; Foresman, J. B.; Ortiz, J. V.; Cui, Q.; Baboul, A. G.; Clifford, S.; Cioslowski, J.; Stefanov, B. B.; Liu, G.; Liashenko, A.; Piskorz, P.; Komaromi, I.; Martin, R. L.; Fox, D. J.; Keith, T.; Al-Laham, M. A.; Peng, C. Y.; Nanayakkara, A.; Challacombe, M.; Gill, P. M. W.; Johnson, B.; Chen, W.; Wong, M. W.; Gonzalez, C.; Pople, J. A. *Gaussian 03*, revision C.01; Gaussian, Inc.: Wallingford, CT, 2004.

(45) Jacox, M. E. *J. Phys. Chem. Ref. Data* **1994**, 3.

(46) Kawaguchi, K. *J. Chem. Phys.* **1992**, *96*, 3411.

(47) Shimanouchi, T. Molecular Vibrational Frequencies. In *NIST Chemistry WebBook*, NIST Standard Reference Database Number 69; Linstrom, P. J., Mallard, W. G., Eds.; National Institute of Standards and Technology: Gaithersburg MD, 20899, http://webbook.nist.gov (retrieved December 11, 2008).

(48) Chase, M. W. NIST-JANAF Tables, 4th ed. *J. Phys. Chem. Ref. Data* **1998**.

(49) Karton, A.; Martin, J. M. L. *J. Phys. Chem. A* **2007**, *111*, 5936.

(50) Storms, E.; Mueller, B. *J. Phys. Chem.* **1977**, *81*, 318.

(51) Ruscic, B.; Mayhew, C. A.; Berkowitz, J. *J. Chem. Phys.* **1988**, *88*, 5580.

(52) Martin, J. M. L.; Taylor, P. R. *J. Phys. Chem. A* **1998**, *102*, 2995.

(53) Cox, J. D.; Wagman, D. D.; Medvedev, V. A. *CODATA Key Values for Thermodynamics*; Hemisphere Publishing Corp.: New York, 1989.

(54) Gurvich, L. V.; Veyts, I. V.; Alcock, C. B. *Thermodynamic Properties of Individual Substances*; Begell House: New York, 1996; Vol. 3.

(55) Curtiss, L. A.; Raghavachari, K.; Redfern, P. C.; Pople, J. A. *J. Chem. Phys.* **1997**, *106*, 1063.

(56) Curtis, L. A.; Redfern, P. C.; Raghavachari, K.; Rassolov, V.; Pople, J. A. *J. Chem. Phys.* **1999**, *110*, 4703.

(57) Harmony, M. D.; Laurie, V. W.; Kuczkowski, R. L.; Schwendeman, R. H.; Ramsey, D. A.; Lovas, F. J.; Lafferty, W. J.; Maki, A. G. *J. Phys. Chem. Ref. Data* **1979**, *8*, 619.

(58) Dixon, D. A.; Arduengo, A. J., III. *J. Phys. Chem. A* **2006**, *110*, 1968.

(59) Gutowski, K. E.; Rogers, R. D.; Dixon, D. A. *J. Phys. Chem. A* **2006**, *110*, 11890.

(60) Lee, T. J.; Taylor, P. R. *Int. J. Quantum Chem. Symp.* **1989**, *23*, 199.

(61) Pedley, J. B. *Thermochemical Data and Structures of Organic Compounds*; TRC Data Series; Thermodynamics Research Center, Texas A&M University: College Station, TX, 1994.

(62) Wagman, D. D.; Evans, W. H.; Parker, V. B.; Schumm, R. H.; Halow, I.; Bailey, S. M.; Churley, K. L.; Nuttall, R. L. *J. Phys. Chem. Ref. Data* **1982**, *11*.

(63) Lias, S. G.; Bartmess, J. E.; Liebman, J. F.; Holmes, J. L.; Levin, R. D.; Mallard, W. G. *J. Phys. Chem. Ref. Data* **1988**, *17*.

(64) Cox, J. D.; Pilcher, G. *Thermochemistry of Organic and Organometallic Compounds*; Academic Press: London, 1970.

(65) Guest, M. F.; Pedley, J. B.; Horn, M. *J. Chem. Thermodyn.* **1969**, *1*, 345.

(66) Frenkel, M.; Marsh, K. N.; Wilhoit, R. C.; Kabo, G. J.; Roganov, G. N. *Thermodynamics of Organic Compounds in the Gas State*; TRC Data Series; Thermodynamic Research Center, Texas A&M University: College Station, TX, 1944; Vol. 1.

(67) Haalane, A. *Angew. Chem., Int. Ed. Engl.* **1989**, *28*, 992.

(68) McCoy, R. E.; Bauer, S. H. *J. Am. Chem. Soc.* **1956**, *78*, 2061.

(69) Brown, H. C.; Bartholomay, H., Jr.; Taylor, M. D. *J. Am. Chem. Soc.* **1944**, *66*, 435.

(70) Jonas, V.; Frenking, G.; Reetz, M. *J. Am. Chem. Soc.* **1994**, *116*, 8741.

(71) Sana, M.; Leroy, G.; Wilante, C. *Organometallics* **1992**, *11*, 781.

(72) Beall, H.; Bushwell, Ch. *Chem. Rev.* **1973**, *73*, 465.

(73) Nguyen, M. T.; Matus, M. H.; Lester, W. A., Jr.; Dixon, D. A. *J. Phys. Chem. A* **2008**, *112*, 2082.

(74) Eades, R. A.; Well, D. A.; Dixon, D. A.; Douglass, C. H., Jr. *J. Phys. Chem.* **1981**, *85*, 976.

(75) (a) Becke, A. D. *J. Chem. Phys.* **1993**, *98*, 5648. (b) Lee, C.; Yang, W.; Parr, R. G. *Phys. Rev. B* **1988**, *37*, 785.

(76) Godbout, N.; Salahub, D. R.; Andzelm, J.; Wimmer, E. *Can. J. Chem.* **1992**, *70*, 560.

(77) Feller, D.; Peterson, K. A.; Dixon, D. A. *J. Chem. Phys.* **2008**, *129*, 204015.

(78) Brazier, C. R. *J. Mol. Spectrosc.* **1996**, *177*, 90.

(79) Tel'noi, V. I.; Rabinovich, I. B. *Russ. Chem. Rev.* **1980**, *49*, 603. *Engl. Transl.* **1980**, *49*, 1134.

JP902196D